Acta Crystallographica Section D
Biological Crystallography
ISSN 0907-4449

Structure of a mutant $T = 1$ capsid of Sesbania mosaic virus: role of water molecules in capsid architecture and integrity

V. Sangita,[a] P. S. Satheshkumar,[b] H. S. Savithri[b] and M. R. N. Murthy[a]*

[a]Molecular Biophysics Unit, Indian Institute of Science, Bangalore 560 012, India, and [b]Department of Biochemistry, Indian Institute of Science, Bangalore 560 012, India

Correspondence e-mail: mrn@mbu.iisc.ernet.in

Received 29 April 2005
Accepted 27 July 2005

PDB Reference: CP-NΔ31, 1x36, r1x36sf.

Deletion of the N-terminal 31 amino acids from the coat protein (CP) of Sesbania mosaic virus (SeMV) results in the formation of $T = 1$ capsids. The X-ray crystal structure of CP-NΔ31 mutant capsids reveals that the CP adopts a conformation similar to those of other $T = 1$ mutants. The 40 N-terminal residues are disordered in CP-NΔ31. The intersubunit hydrogen bonds closely resemble those of the native capsid. The role of water molecules in the SeMV structure has been analyzed for the first time using the present structure. As many as 139 of the 173 waters per subunit make direct contacts with the protein atoms. The water molecules form a robust scaffold around the capsid, stabilize the loops and provide integrity to the subunit. These waters constitute a network connecting diametrically opposite ends of the subunit. Such waters might act as nodes for conveying signals for assembly or disassembly across a large conformational space. Many water-mediated interactions are observed at various interfaces. The twofold interface, which has the smallest number of protein–protein contacts, is primarily held by water-mediated interactions. The present structure illuminates the role of water molecules in the structure and stability of the capsid and points out their possible significance in assembly.

1. Introduction

Water molecules play a crucial role in both protein structure and function. The availability of a large number of crystal structures of proteins at high resolution has made possible the comparison and analysis of solvent structure within individual classes of proteins (Loris *et al.*, 1994; Sreenivasan & Axelsen, 1992; Krem & Enrico, 1998; Prasad & Suguna, 2002). In these, conserved water molecules have been identified across homologous members in spite of significant variations in the sequence, suggesting functional and/or structural importance of certain water molecules.

Owing to the limited resolution of virus structures, water molecules have largely been excluded from detailed analysis. However, water molecules have been identified in the high-resolution crystal structures of several viruses and their involvement in stabilizing the capsid structure has been pointed out (Larson *et al.*, 1998, 2000; McKenna *et al.*, 1994; Benson *et al.*, 2002). These studies accentuate the need for the detailed study of solvent molecules in crystal structures of viruses.

SeMV is an isometric single-stranded RNA virus that belongs to the family Sobemoviridae (Tamm & Truve, 2000). The amino-terminal arm (N-ARM) of the SeMV coat protein (CP; residues 28–36) is rich in positively charged residues and hence is thought to interact with RNA. This segment is

disordered in all the subunits of the native virus crystal structure. The β-annulus is a hydrogen-bonded structure formed by the ordered N-ARMs of the three *C*-type subunits at the icosahedral threefold axes (Bhuvaneshwari *et al.*, 1995). When a deletion mutant (CP-NΔ31) lacking 31 residues from the N-terminus, including three arginine residues (Arg28–Arg31) of the N-ARM, was expressed in *Escherichia coli*, virus-like particles (VLPs) with a diameter smaller than that of the wild-type particles were formed (Satheshkumar *et al.*, personal communication). In this communication, we present the X-ray crystal structure of CP-NΔ31 capsids. This mutant shows similarities in structure and capsid organization to other mutant $T = 1$ capsids solved previously (Sangita *et al.*, 2004). CP-NΔ31 is the highest resolution structure available for any mutant $T = 1$ capsid. A large number of water molecules were identified in the structure and subjected to detailed analysis.

The present analysis is mainly concerned with probing whether the water molecules occur as integral parts of the viral CP and addressing the contribution of water molecules to the intersubunit contacts at various interfaces. Such water molecules are likely to contribute significantly to the stability of CP and the packing of the subunits at different interfaces. A comparative analysis of water structures in CP-NΔ31 and CP-NΔ65 (Sangita *et al.*, 2004) has also been made. It was observed that the water molecules account for a large number of contacts at intersubunit interfaces. They also contribute to the stability of loops and secondary-structural elements within a subunit. The present analysis points out the importance of identifying and analyzing waters in viral structures.

Table 1
Data-reduction and refinement statistics for CP-NΔ31.

Values in parentheses correspond to the highest resolution shell.

Space group	$P2_12_12_1$
Unit-cell parameters (Å)	
a	193.4
b	313.5
c	321.2
Resolution limits (Å)	20.0–2.7 (2.8–2.7)
Total No. of observations	738517
No. of unique reflections	515695
Completeness (%)	97.9 (96.9)
Multiplicity	1.4 (1.3)
$I/\sigma(I)$	5.0 (2.3)
$R_{\rm merge}$†	10.2 (22.5)
No. of protein atoms per subunit	1463
No. of waters per subunit	173
No. of ions per subunit	1
$R_{\rm work}$ (final) (%)	24.5 (31.1)
$R_{\rm free}$ (final) (%)	24.7 (31.2)
R.m.s.d.s	
Bond lengths (Å)	0.005
Bond angles (°)	1.3
Dihedral angles (°)	25.2
Improper angles (°)	0.77
Average temperature factors (Å^2)	
Protein atoms	14.5
Waters	23.5
Calcium	11.7
Ramachandran statistics	
Most favoured region (%)	90.1
Additionally allowed region (%)	9.9
Generously allowed region (%)	0.0
Disallowed region (%)	0.0

† $R_{\rm merge} = \sum_{hkl} |I - \langle I \rangle| / \sum I$, where I is the observed intensity and $\langle I \rangle$ is the average intensity from observations of symmetry-related reflections.

2. Materials and methods

The purified CP-NΔ31 capsids were used for crystallization at a concentration of 6 mg ml^{-1} using the hanging-drop vapour-diffusion method. Good crystals were obtained in 0.1 *M* HEPES buffer pH 7.5 containing 6%(*w*/*v*) PEG 3350, 0.2 *M* $MgCl_2$ and 0.1%(*v*/*v*) isopropanol. The crystals belonged to space group $P2_12_12_1$ and contained a full VLP in the asymmetric unit.

X-ray diffraction data were collected to a resolution of 2.7 Å from a single crystal using a MAR345 imaging-plate detector mounted on a Rigaku RU-200 rotating-anode generator equipped with a 200 µm focal cup. The data were collected at 100 K using 20%(*v*/*v*) glycerol as the cryoprotectant. The crystal-to-detector distance was set to 260 mm and the images were collected with an oscillation angle of 0.25°. The frames were processed and scaled using *DENZO* and *SCALEPACK*, respectively, from the *HKL* suite of programs (Otwinowski & Minor, 1997). The data-collection and reduction statistics are presented in Table 1.

Self-rotation functions (Tong & Rossmann, 1990) computed for κ = 72, 120 and 180° hemispheres confirmed the icosahedral symmetry of the CP-NΔ31 capsids. The molecular-replacement program *AMoRe* (Navaza & Saludjian, 1997) was used to obtain an initial solution to the structure. Reflections in the resolution range 12–5.5 Å and a polyalanine model of the CP-NΔ65 capsid were used for the molecular-replacement calculations. The best solution had a correlation coefficient of 84.9% and an *R* factor of 28.3%. The *AMoRe* coordinates were subjected to 20 cycles of rigid-body refinement, after which Fourier maps were calculated. Strict NCS constraints corresponding to the icosahedral symmetry were applied throughout the refinement. A molecular model was built into the electron-density map using *O* (Jones *et al.*, 1991). After the first round of model building, 20 cycles of rigid-body and 300 cycles of positional refinement were carried out using *CNS* v.1.1 with the MLF target (Brünger *et al.*, 1998). At the end of the refinement, simulated annealing was performed with a starting temperature of 3000 K. Subsequently, every cycle of model building was followed by refinement using *CNS* v.1.1. The final $R_{\rm work}$ and $R_{\rm free}$ were 24.5 and 24.7%, respectively. It should be noted that $R_{\rm free}$ does not have the usual significance owing to the high NCS. The other refinement statistics are presented in Table 1. The quality of the final model was assessed using the program *PROCHECK* (Laskowski *et al.*, 1993).

Waters which make contact with the protein atoms, referred to as the primary hydration waters, were identified using the *CONTACT* module of *CCP*4 (Collaborative Computational Project, Number 4, 1994). Superposition of the structures was achieved using the program *ALIGN* (Cohen, 1997). The 3.0 Å crystal structure of CP-NΔ65 (PDB code 1vak) was aligned with the structure of CP-NΔ31 and the aligned structures along with their primary hydration waters were used to find

Table 2
Contacts made by the buried waters of CP-N31.

	Contacting residues					
Buried waters	Residue 1	Residue 2	Residue 3	Residue 4	Residue 5	Residue 6
w282	Tyr118 OH	Pro206 O	Leu227 O	w316	—	—
w316	Tyr102 N	Lys208 N	Lys208 O	w282	—	—
w317	Met147 N	Tyr145 O	Thr225 N	Thr225 OG1	w340	w381
w349	Ala112 O	Lys117 O	Trp115 O	—	—	—
w360	Tyr125 OH	Leu98 O	—	—	—	—
w376	Gly172 O	Tyr127 O	Ile191 N	Ile191 O	—	—
w388	Thr89 N	Thr89 OG1	Ser91 O	Trp330 O	Leu236 O	—
w391	Thr283 OG	Thr126 OG	Arg124 O	Thr126 N	Tyr251 O	Thr253 N

the conserved waters. Waters of individual structures that were within 1.8 Å of one another after superposition and made at least one common hydrogen bond to the protein main-chain atom were considered as conserved or invariant waters.

Cavities or pockets in the viral structures were identified using the web-based server *CASTp* (Binkowski *et al.*, 2003) and only those pockets that exceeded 50 Å^3 in size were considered for further analysis and were visually examined for the presence of water molecules. The surface accessibilities of the primary hydration waters were computed in the presence of the protein atoms using the molecular-surface package *NACCESS* (Hubbard & Thornton, 1993). The probe radius was taken to be 1.4 Å. Waters with an accessible surface area of less than 1.0 Å^2 were considered to be internal waters. Buried waters at various viral interfaces were identified by picking those waters that showed an accessibility of more than 30% in the monomeric state of the subunit and whose accessibility dropped to less than 8% in the presence of the neighbouring subunit. The buried surface areas at the interfaces were calculated using the program *NACCESS* (Hubbard & Thornton, 1993). *MOLSCRIPT* (Kraulis, 1991) and *BOBSCRIPT* (Esnouf, 1997) were used to generate the figures and *RASTER3D* (Merritt & Bacon, 1997) was used to render them to TIF format.

3. Results

3.1. Quality of the model

The final refined model was reasonable, with about 90% of residues in the most favourable region of the Ramachandran plot (Ramachandran & Sasisekharan, 1968). The r.m.s.d.s of bond lengths and bond angles were also well within the allowed cutoff. The initial model was built into a map calculated from a polyalanine chain of CP-NΔ65. There were almost no breaks in the main chain and, except for Arg183 and Ser185, the side chains of rest of the residues could be built without ambiguity (Fig. 1). Density for water molecules were identified at 3.0 positive σ in the difference Fourier map and 1.0σ cutoff in the Fourier map. A total of 173 water molecules were identified per subunit for CP-NΔ31. There was a strong density corresponding to a calcium ion at the intersubunit interface of threefold-related subunits. There are two strong densities at the fivefold axis, of which one is close to Trp170, as observed in the native and other $T = 1$ mutant capsid structures; the other is close to Asp186. A water molecule has been modelled into the latter. At the threefold axis there is a small positive density which was modelled as a water molecule.

3.2. Positions of water molecules

As many as 139 water molecules were identified in the primary hydration shell of CP-NΔ31 (Fig. 2). There were 34 secondary hydration waters that only make contacts with other water molecules. The number of contacts of water molecules with main-chain O, main-chain N, side-chain O and side-chain N atoms are 92, 56, 69 and 32, respectively. Eight buried waters were identified per CP subunit. These buried waters are in close contact with adjacent residues, mostly involving the main-chain N and O atoms (Table 2).

The buried water molecules are not localized in a particular region of the CP, but are spread across the subunit. Although

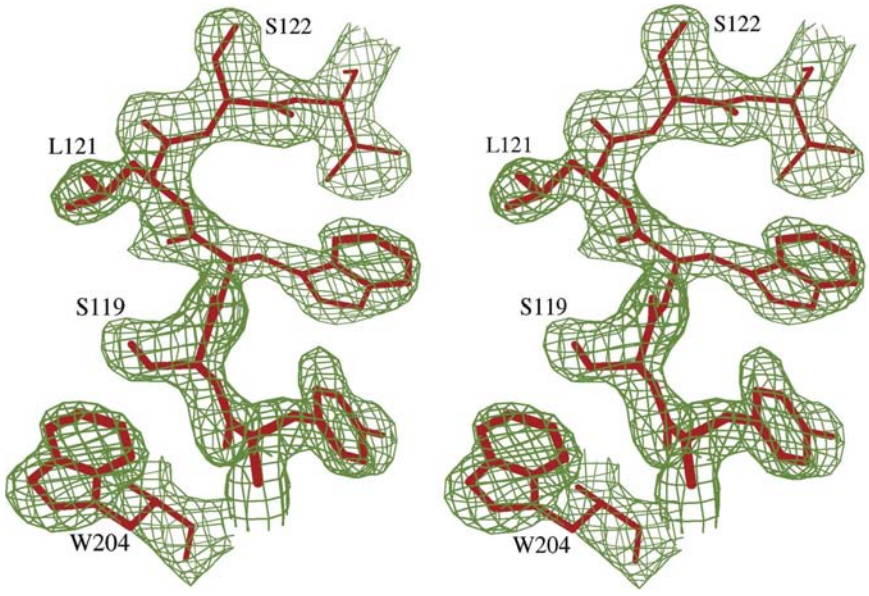

Figure 1
Quality of the electron-density map of CP-NΔ31 contoured at 1.4σ cutoff.

the buried waters appear to be spatially isolated, they are interconnected through a continuous network of hydrogen bonds involving the main-chain atoms of the β-strands that flank them (Fig. 3*a*). This network emanates from the calcium ions and connects different regions of the CP subunit. There are many other water molecules that are closely associated with the calcium-binding loop and stabilize its structure (Fig. 3*b*).

A total of five pockets (named P19–P23) with volumes of more than 50 Å^3 were selected for the analysis. These pockets were further classified on the basis of the number of openings to the solvent. The P20, P21, P22 and P23 pockets had two openings to the solvent, while P19 had only one. There was at least one water associated with each of these pockets. The positions of the water with respect to the opening of the pocket was varied and hence these waters showed differences in their accessibilities. One of the pockets, P23, which was located between βB and βH, shows hydrophobic character. In this pocket, the hydrophobic side chains of Ile234, Ile250, Ile186 and Leu232 face the pocket. The other pockets are not hydrophobic. A totally buried water, w360, occurs close to the hydrophobic pocket P23. Buried waters might play an important role in stabilizing the CP structure.

3.3. Waters at the fivefold

The fivefold interface has the maximum buried surface area of all the interfaces (~2900 Å^2). Many charged and polar residues at this interface contribute to the large number of hydrogen bonds. There is a salt bridge between Arg249 of one subunit and Asp238 of its fivefold partner. There are 24 water molecules at this interface, accounting for ~50% of total contacts. Of these waters, five are completely buried. There are eight water–water contacts and 24 water–protein contacts at each of the fivefold interfaces. Of the waters observed near the fivefold axis, w448 lies exactly on the axis. Previously, in tobacco necrosis virus (TNV), a similar water molecule was reported to be present on the fivefold axis (Oda *et al.*, 2000). However, in other sobemoviruses such a water molecule has not been observed. In CP-NΔ31, a total of five water molecules (w392) form a ring ~23 Å from the internal opening of the fivefold axis (Fig. 4). These water molecules are within a favourable contact distance of 3.5 Å from one another. Ten more waters (w326 and w416 from each fivefold partner) occur at a larger distance from the centre of the fivefold axis and make hydrogen bonds with the surrounding residues.

3.4. Waters at the threefold

The threefold interface has a buried surface area of ~2800 Å^2 and is held together by a large number of hydrogen bonds and a salt bridge between Asp149 and Lys208 which joins two loops of threefold-related subunits. This interface also houses a calcium ion, which adopts an octahedral

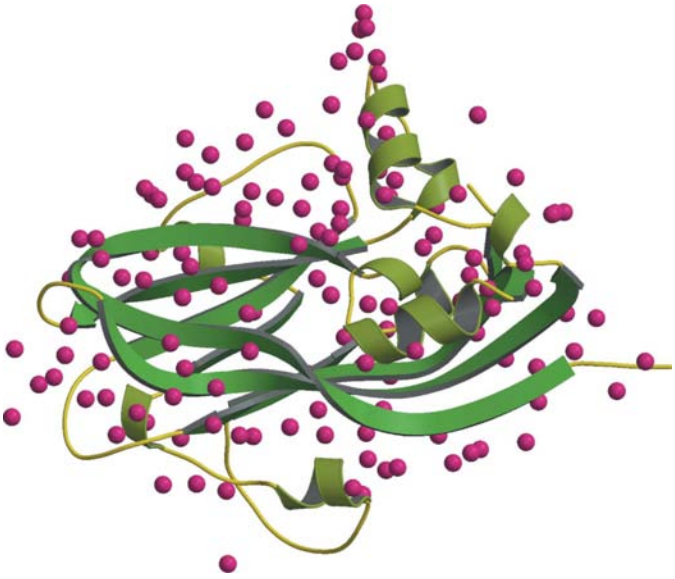

Figure 2
Primary hydration waters of CP-NΔ31.

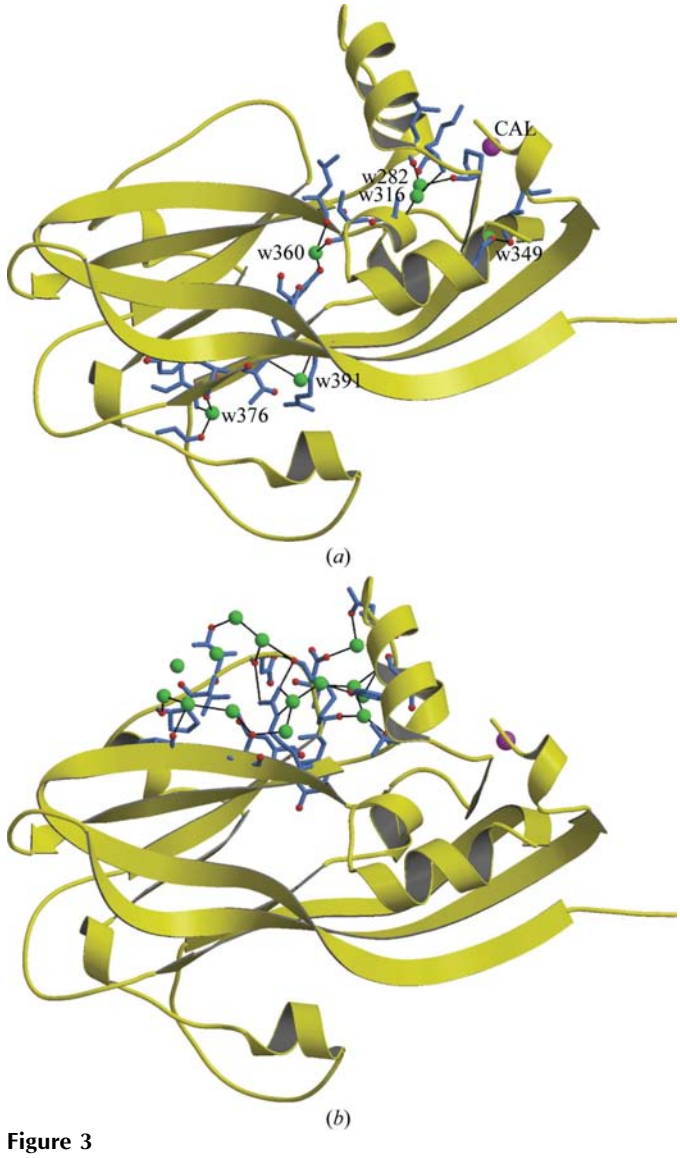

Figure 3
(*a*) Hydrogen-bonded network of protein atoms and buried waters across the CP subunit. (*b*) Hydrogen-bonded network of protein atoms and waters associated with the calcium-binding loop.

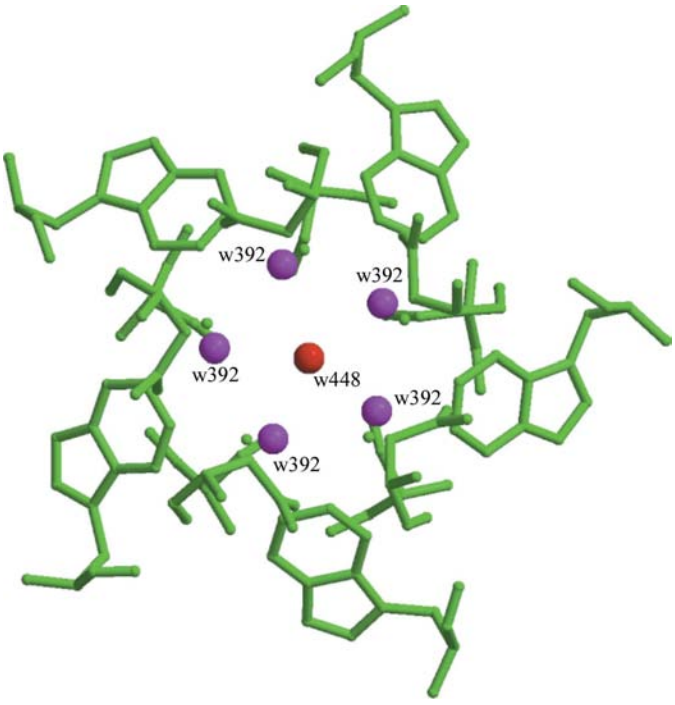

Figure 4
Arrangement of water molecules at the fivefold axis in CP-NΔ31.

geometry. The ligands include Asp146, Asp149 and a water molecule (w415) from one subunit and Tyr207, Asn267 and Asn268 from the neighbouring subunit. A total of 28 water molecules occur at the interface and contribute to 60 contacts, of which 23 are water–water contacts and 37 are protein–water contacts. Eight buried water molecules are observed at this interface.

The threefold axis in CP-NΔ31 features a density that lies at a distance of ∼6 Å from the interior end and is flanked by Lys202 and Pro226 emanating from the threefold-related subunits. A corresponding large density could be observed in native SeMV, which was proposed to correspond to a bound anion. However, in CP-NΔ31 a water molecule (w447) has been modelled into this density. This water comes within contacting distance of a set of three waters (w284) related by threefold symmetry, which in turn are held in place by the neighbouring NZ of Lys202 and a water molecule, w353 (Fig. 5).

3.5. Waters at the twofold

The twofold interface in CP-NΔ31 has the lowest buried surface area (∼1100 Å^2). The T = 1 mutants only have icosahedral twofold interfaces compared with the two types of interfaces in T = 3 capsids: quasi and icosahedral. However, the icosahedral twofold interface of T = 1 capsids is similar to the quasi-twofold interface of the T = 3 capsids in terms of organization and intersubunit interactions. Only two protein–protein contacts are observed at this interface, one between Trp107 NE1 and Asn114 O and the other between Thr262 O and Trp107 NE1. This is a consequence of the lack of polar side chains to mediate hydrogen bonds. In contrast, a large number of hydrophobic groups face the twofold interface. Nevertheless, 28 water molecules are observed at the twofold interface (Fig. 6) and mediate 16 water–water and ten water–protein contacts. Earlier structural studies with T = 1 capsids of SeMV revealed four water-mediated bridges between the main-chain N and O atoms of residues Val76, Leu77 and Thr78 of one subunit and the same atoms of the twofold-related subunit (Sangita *et al.*, 2004). In addition to these, in CP-NΔ31 a few additional water molecules are identified at the dimeric interface. The water molecules at the twofold axis seem to mimic the βA strands of the C subunits (Fig. 6) at the icosahedral CC6 interface of the native virus, which is absent in the mutant capsids. Two buried waters are observed at the twofold interface.

3.6. Invariant waters

A set of 54 invariant waters (Fig. 7) were identified among the mutant T = 1 capsids, of which 39 could be considered as intrasubunit waters and 15 as intersubunit waters. The intrasubunit invariant buried waters include w282, w316, w317, w360 and w388. The intrasubunit invariant waters (w282 and w316) that are buried are positioned close to the calcium-binding site (CBS). Among the intersubunit interfaces, the largest numbers of invariant waters occur at the fivefold, with seven invariant waters. The threefold and twofold interfaces house four invariant waters each. The two invariant waters at the twofold interface are associated with the amino-terminal residues and bridge the βB strand of twofold-related subunits. One of the buried invariant waters is associated with C-terminal residue 264. Overall, many invariant waters seem to be closely associated with the CBS and the loops, implying that the water molecules are probably essential to maintain their conformations.

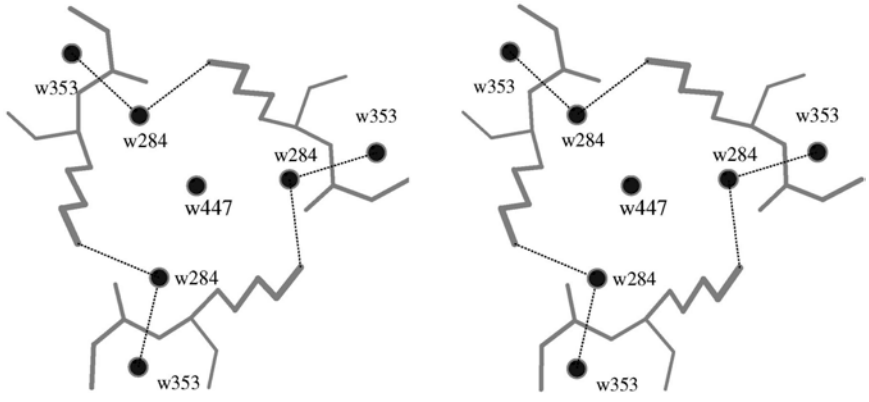

Figure 5
Stereoview of the arrangement of water molecules at the threefold axis in CP-NΔ31.

4. Discussion

Deletion of 31 amino acids from the N-terminus of SeMV CP, which includes part of the N-ARM, led to the formation of smaller $T = 1$ particles similar to those formed by the deletion of 36 and 65 amino acids (Lokesh *et al.*, 2002). The rationale behind the construction of CP-NΔ31 mutant was to investigate whether retention of the first three arginines of the N-ARM alone would be sufficient to form $T = 3$ capsids. However, the CP-NΔ31 mutant formed only a $T = 1$ shell, implying that the length of the amino-terminus to a major extent determines the particle size in SeMV.

Many common waters were identified in the mutant $T = 1$ capsids of SeMV, which are either associated with loops or are totally buried, implying their role in subunit architecture. As many as 139 out of the 173 waters that were modelled per subunit make direct contacts with the protein atoms. There are several completely buried water molecules in CP-NΔ31, suggesting that they constitute an integral part of the CP subunit. In satellite tobacco mosaic virus (STMV), 20% of water molecules were implicated in bridging distant hydrogen-bonding groups (Larson *et al.*, 1998). Similarly, in the P3 trimer of bacteriophage PRD1, an extensive network of water molecules was observed and implicated in its stabilization (Benson *et al.*, 2002). Likewise, in CP-NΔ31 the water molecules are involved in a network of hydrogen bonds connecting diametrically opposite ends of the subunit. Such waters might convey structural changes across the subunits and hence could be important for assembly and disassembly. A strategy for the disassembly of this virus is believed to be the release of calcium ions prompted by the change in pH inside the plant cell. Such a change could possibly have implications for the water-mediated bonds, as these bonds run from the bound ion or its ligands through the subunit.

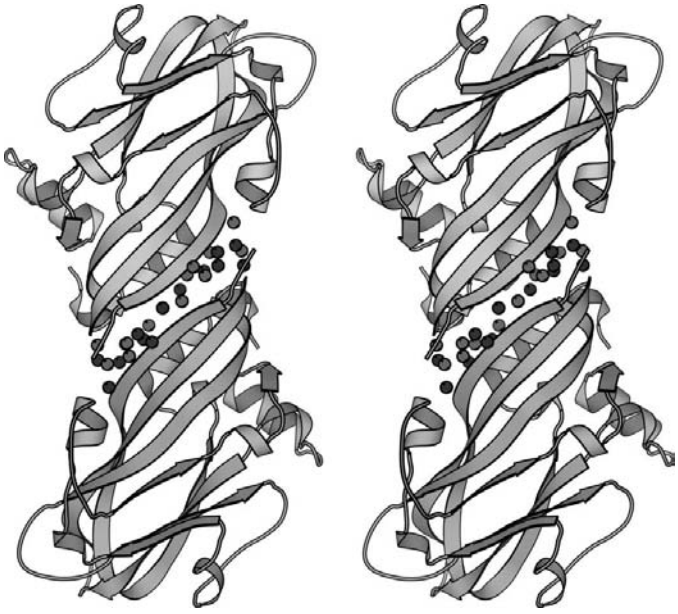

Figure 6
Stereoview of arrangement of water molecules at the twofold of CP-NΔ31.

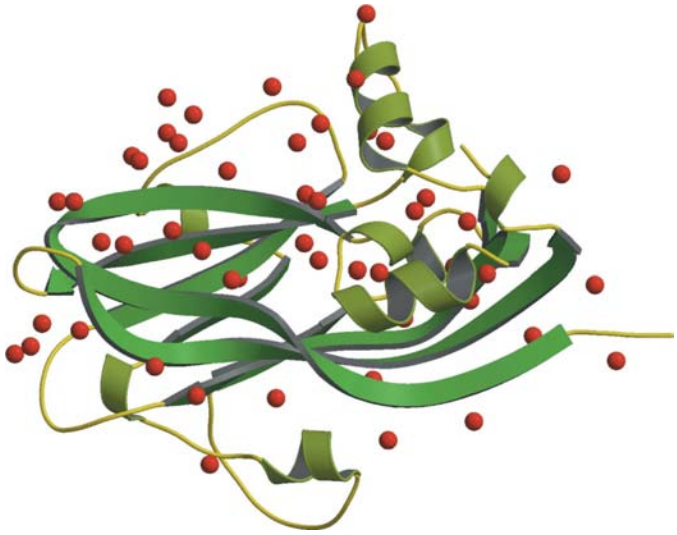

Figure 7
Positions of invariant water molecules in SeMV.

Many water molecules appear to be integral components of the intersubunit interfaces. The interfacial water molecules were implicated in stabilizing spike–capsid interactions in bacteriophage φX174 (McKenna *et al.*, 1994). In desmodium yellow mottle virus, a large number of water molecules were shown to be important in stabilizing intersubunit associations (Larson *et al.*, 2000). Similarly, in CP-NΔ31 the fivefold and threefold interfaces house a large number of water molecules that contribute to the stability of these interfaces. However, the most interesting scenario is the water structure at the twofold interface, as most of the intersubunit interactions here are a result of hydration. The water molecules at the twofold interfaces of the recombinant $T = 1$ capsids appear to mimic the β-structure formed by the *βA* strands of the *C* subunits of $T = 3$ SeMV. Water structure is probably more easily altered than protein conformation. As $T = 3$ capsids have to form two distinct twofold-related interactions (quasi- and icosahedral twofolds), the changes at the interface may be accommodated more readily by changes in hydration rather than changes in protein conformation. This might be the explanation for the more significant role of water molecules observed at the twofold interface in CP-NΔ31.

This project was supported by the Department of Science and Technology (DST) and Department of Biotechnology (DBT), India. The intensity data were collected at the X-ray Facility for Structural Biology at the Molecular Biophysics Unit, Indian Institute of Science, Bangalore, India supported by the DST and the DBT. Facilities at the Supercomputer Education and Research Centre are gratefully acknowledged. VS and PSS thank CSIR, India for financial support.

References

Benson, S. D., Bamford, J. K. H., Bamford, D. H. & Burnett, R. M. (2002). *Acta Cryst.* D**58**, 39–59.
Bhuvaneshwari, M., Subramanya, H. S., Gopinath, K., Savithri, H. S., Nayudu, M. V. & Murthy, M. R. N. (1995). *Structure*, **3**, 1021–1030.

Binkowski, T. A., Naghibzadeh, S. & Liang, J. (2003). *Nucleic Acids Res.* **31**, 3352–3355.
Brünger, A. T., Adams, P. D., Clore, G. M., DeLano, W. L., Gros, P., Grosse-Kunstleve, R. W., Jiang, J.-S., Kuszewski, J., Nilges, M., Pannu, N. S., Read, R. J., Rice, L. M., Simonson, T. & Warren, G. L. (1998). *Acta Cryst.* D**54**, 905–921.
Cohen, G. E. (1997). *J. Appl. Cryst.* **30**, 1160–1161.
Collaborative Computational Project, Number 4 (1994). *Acta Cryst.* D**50**, 760–763.
Esnouf, R. M. (1997). *J. Mol. Graph.* **15**, 132–134.
Hubbard, S. J. & Thornton, J. M. (1993). *NACCESS.* Department of Biochemistry and Molecular Biology, University College, London.
Jones, T. A., Zou, J. Y., Cowan, S. W. & Kjeldgaard, M. (1991). *Acta Cryst.* A**47**, 110–119.
Kraulis, P. J. (1991). *J. Appl. Cryst.* **24**, 946–950.
Krem, M. M. & Enrico, D. C. (1998). *Proteins*, **30**, 34–42.
Larson, S. B., Day, J., Canady, M. A., Greenwood, A. & McPherson, A. (2000). *J. Mol. Biol.* **301**, 625–642.
Larson, S. B., Day, J., Greenwood, A. & McPherson, A. (1998). *J. Mol. Biol.* **277**, 37–59.
Laskowski, R. A., MacArthur, M. W., Moss, D. S. & Thornton, J. M. (1993). *J. Appl. Cryst.* **26**, 283–291.
Lokesh, G. L., Gowri, T. D., Satheshkumar, P. S., Murthy, M. R. & Savithri, H. S. (2002). *Virology*, **292**, 211–223.
Loris, R., Stas, P. P. G. & Wyns, L. (1994). *J. Biol. Chem.* **269**, 26722–26733.
McKenna, R., Ilag, L. L. & Rossmann, M. G. (1994). *J. Mol. Biol.* **237**, 517–543.
Merritt, E. A. & Bacon, D. J. (1997). *Methods Enzymol.* **277**, 505–524.
Navaza, J. & Saludjian, P. (1997). *Methods Enzymol.* **276**, 581–593.
Oda, Y., Saeki, K., Takahashi, Y., Maeda, T., Naitow, H., Tsukihara, T. & Fukuyama, K. (2000). *J. Mol. Biol.* **300**, 153–169.
Otwinowski, Z. & Minor, W. (1997). *Methods Enzymol.* **276**, 307–326.
Prasad, B. V. L. S. & Suguna, K. (2002). *Acta Cryst.* D**58**, 250–259.
Ramachandran, G. N. & Sasisekharan, V. (1968). *Adv. Protein Chem.* **23**, 283–438.
Sangita, V., Lokesh, G. L., Satheshkumar, P. S., Vijay, C. S., Saravanan, V., Savithri, H. S. & Murthy, M. R. (2004). *J. Mol. Biol.* **342**, 987–999.
Sreenivasan, U. & Axelsen, P. H. (1992). *Biochemistry*, **31**, 12785–12791.
Tamm, T. & Truve, E. (2000). *J. Virol.* **74**, 6231–6241.
Tong, L. & Rossmann, M. G. (1990). *Acta Cryst.* A**46**, 783–792.